Chen et al., Supplementary Fig. 1

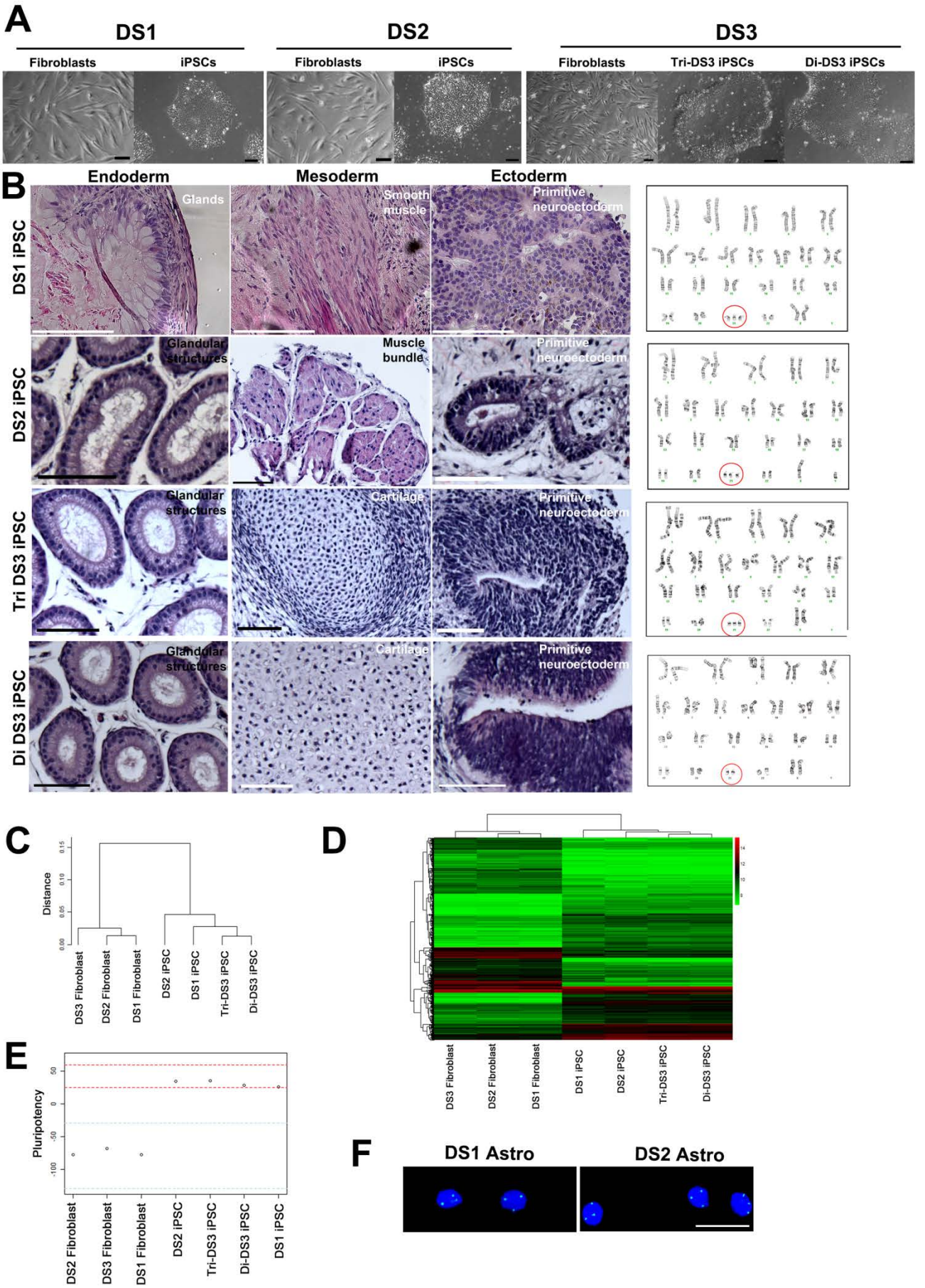

Supplementary Figure 1. Characterization of DS iPSCs.

(A) Bright-field images showing the morphology of fibroblasts and iPSCs from patient DS1, DS2 and DS3. Scale bars represent 100 μm. (B) Representative images showing teratoma formation and karyotypes of DS iPSCs. Hematoxylin and eosin staining of teratomas derived from DS iPSC lines show tissues representative of three major germ layers: ectoderm, mesoderm and endoderm. Scale bars represent 100 μm. The HSA21 are highlighted in red circles. (C) Dendrogram shows that all three fibroblasts cluster together and all iPSCs cluster together despite one of the iPSC lines Di-DS3 has lost the extra HSA21 during culture. Distance is based on Person correlations. (D) Heatmap of differentially expressed genes (≥ 2 folds, $p < 0.05$) in DS iPSCs and fibroblasts. Red color indicates genes with higher expression and green color indicates genes with lower expression. Distinct gene expression pattern can be seen between fibroblasts and iPSCs. (E) Pluritest performed at www.PluriTest.org. Illumina microarray data was uploaded to the PluriTest website and pluripotency score of each cell line was calculated. The three fibroblast lines DS1, DS2 and DS3 fibroblasts have negative pluripotency scores (-77.735, -67.937, and -77.698) and fall between the two blue dotted lines, indicating that they are not pluripotent. In contrast, all four DS iPSC lines have positive pluripotency scores (DS1, 25.763; DS2, 35.051; Tri-DS3, 35.585, and Di-DS3 28.565), and are plotted between two red dotted lines, indicating that they are pluripotent. (F) FISH analysis confirms that DS1 and 2 astroglia maintain trisomic HSA21 stably. Scale bar represents 50 μm.

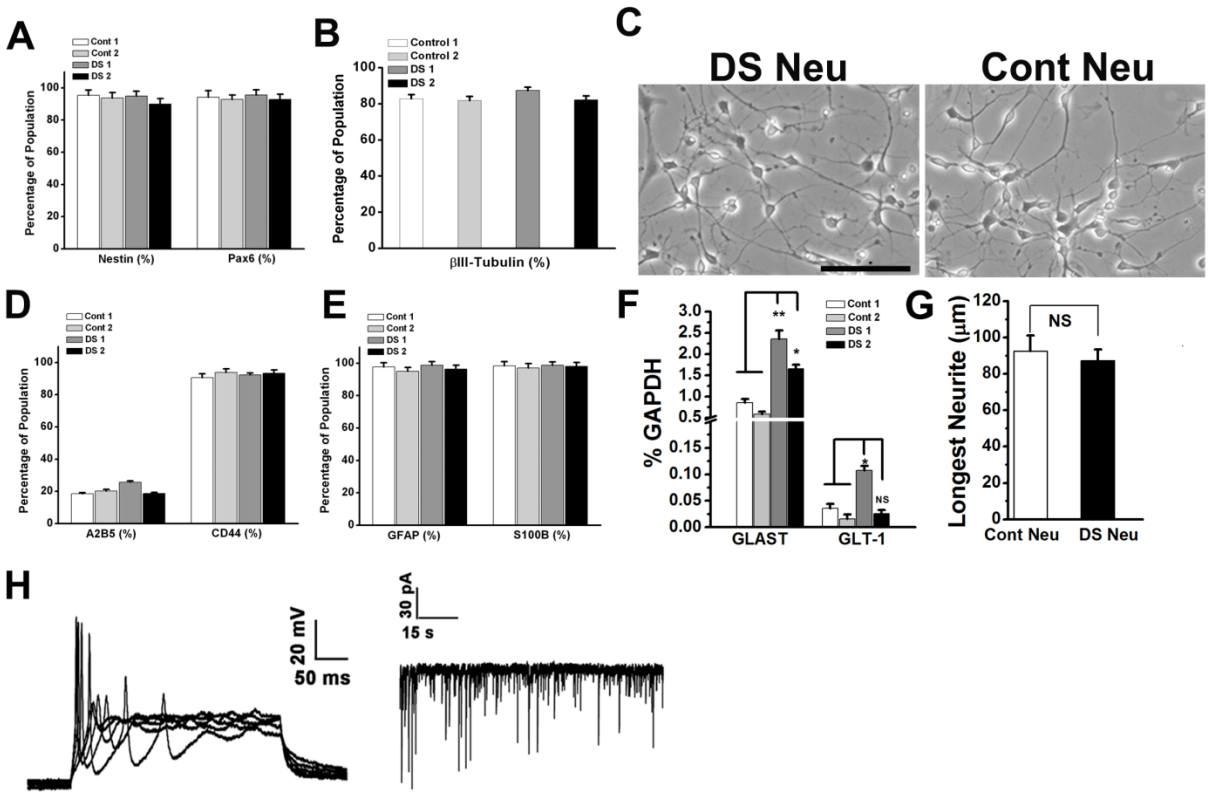

Supplementary Figure 2. Characterization of DS neurons and astroglia.

(A and B) The induction efficiency of NPCs and βIII-tubulin+ neurons from DS iPSC is similar to normal control. (C) Representative bright-field images of control and DS neurons under directed neuronal differentiation condition. Scale bar represents 50 μm. (D and E) Both control and DS iPSCs give rise to astroglia at similar efficiency. (F) Representative bright-field images of control astroglia and DS astroglia. Scale bar represents 50 μm. (G) Quantitative PCR analysis showing the expression of GLAST and GLT-1 in control and DS astroglia. One-way ANOVA test, * $p < 0.05$, ** $p < 0.01$, and NS represents no significant difference. n = 3-4 for each cell line. (H) Quantification of pooled data from control and DS neurons showing the length of the longest neurites of neurons under directed neuronal differentiation conditions (n = 10 from each cell line). Note that control neurons are morphologically undistinguishable from DS neurons. (I) 10-week-old DS neurons fire action potentials and exhibit spontaneous postsynaptic currents.

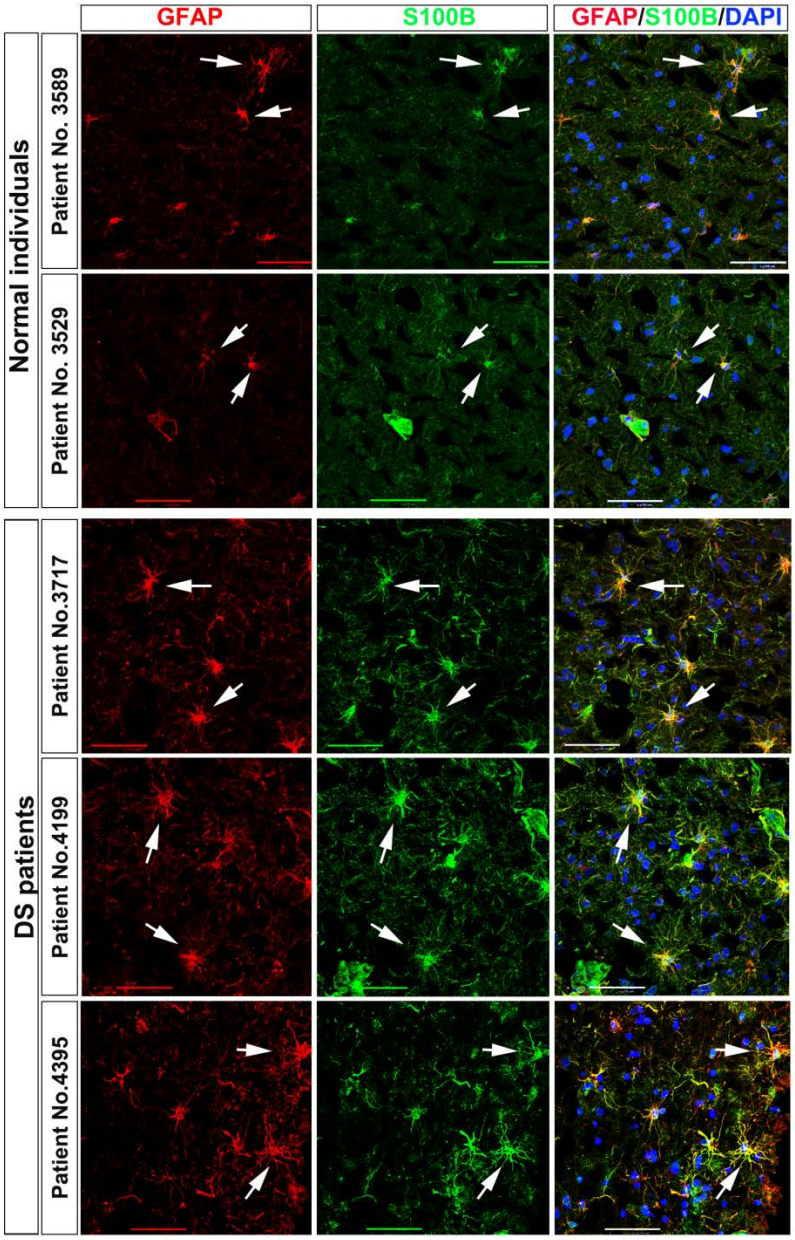

Supplementary Figure 3. Expression of GFAP and S100B in the DS and normal human brain tissues.

Representative images showing the expression of GFAP and S100B in the frontal cerebral cortex of the brain tissues from two normal individuals and three DS patients. Note the higher immunoreactivity of GFAP/S100B and an activated morphology of astrocytes in the DS brain tissues, compared to the normal brain tissues. Scale bars represent 50 μm. Arrows indicate the astrocytes positive for GFAP and S100B.

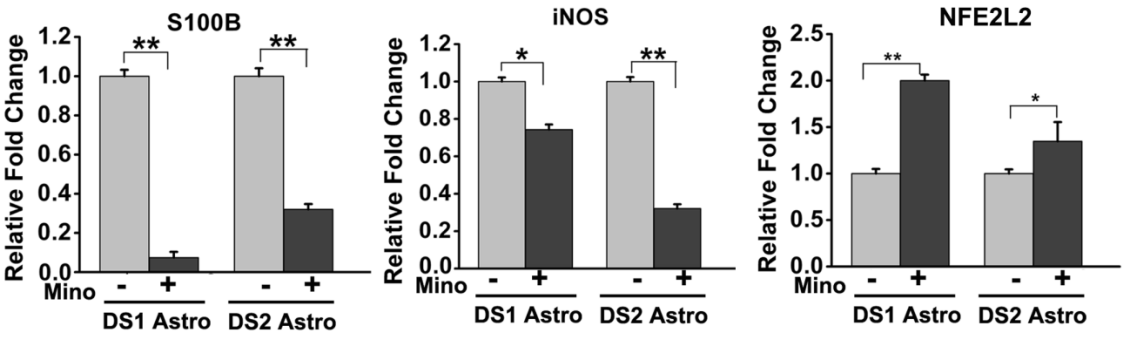

Supplementary Figure 4. Correction of pathological phenotypes of DS astroglia by minocycline.

Quantitative PCR analysis showing the expression of S100B, iNOS and NFE2L2 mRNA in DS1 and 2 astroglia with or without treatment of minocycline. Student t test, * $p < 0.05$ and ** $p < 0.01$.

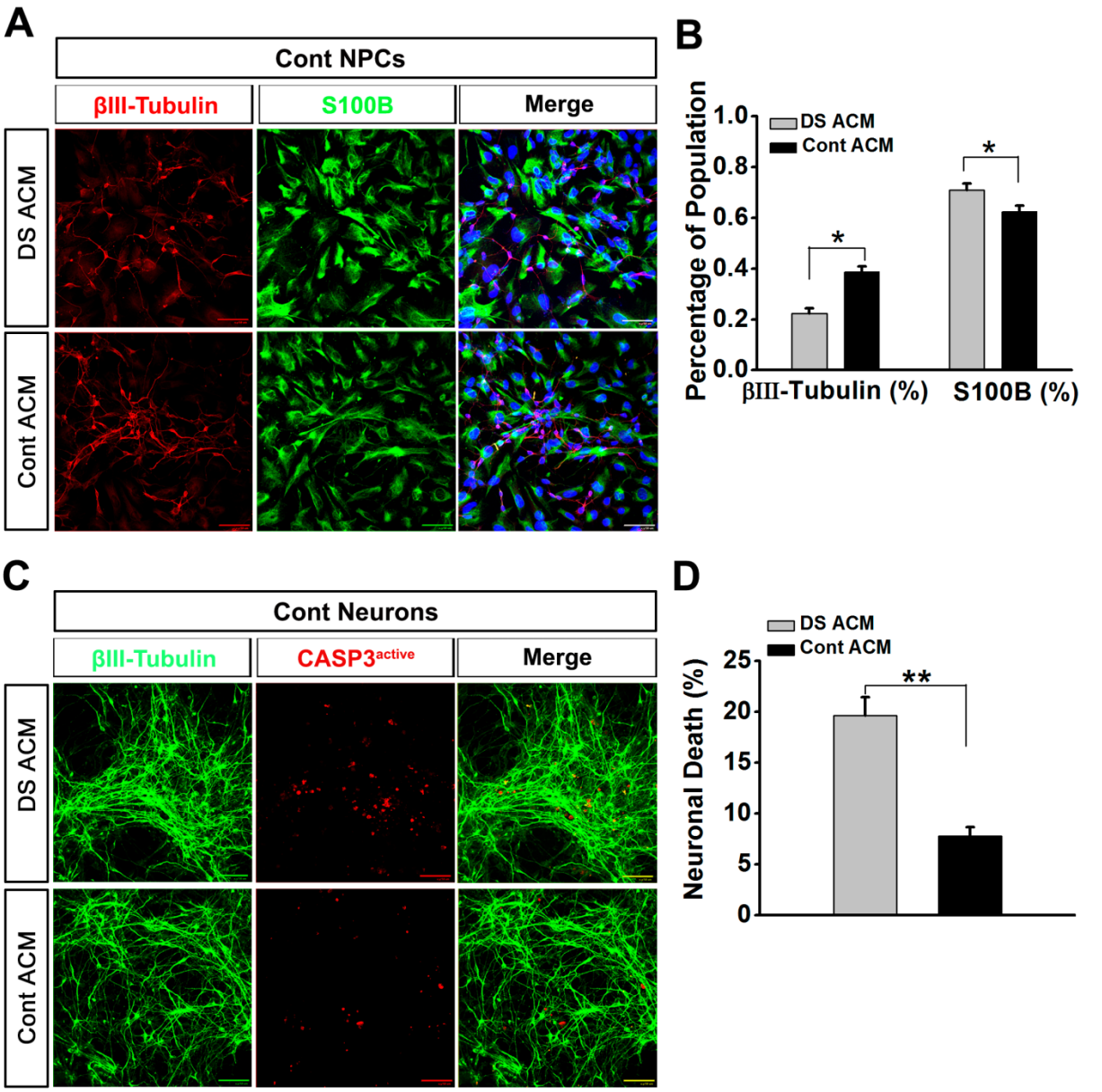

Supplementary Figure 5. The effects of DS astroglia on the Cont NPC differentiation and Cont neuron survival.

(A and B) Representatives and quantification of βIII-tubulin+ neurons and S100B+ astroglia derived from Cont NPCs under spontaneous differentiation condition in the presence of DS ACM and Cont ACM. Student t test, * $p < 0.05$, n =3 for each group. (C and D) Representatives and quantification of βIII-tubulin+ and activated caspase3+ between the groups neurons with different treatment. Student t test, ** $p < 0.01$, n = 3-6 for each group. Scale bars represent 50 μm. Blue, DAPI-stained nuclei.

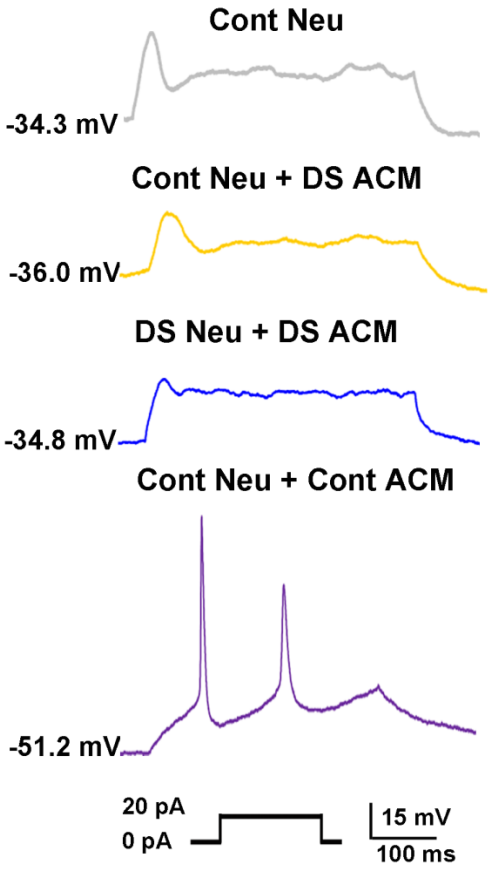

Supplementary Figure 6. The effects of DS astroglia on the action potential firing of DS neurons.

Representative tracing showing at RMP, the action potential firing from Cont neurons alone, Cont neurons fed with DS ACM or Cont ACM, and DS neurons fed with DS ACM.

Chen et al., Supplementary Fig. 7

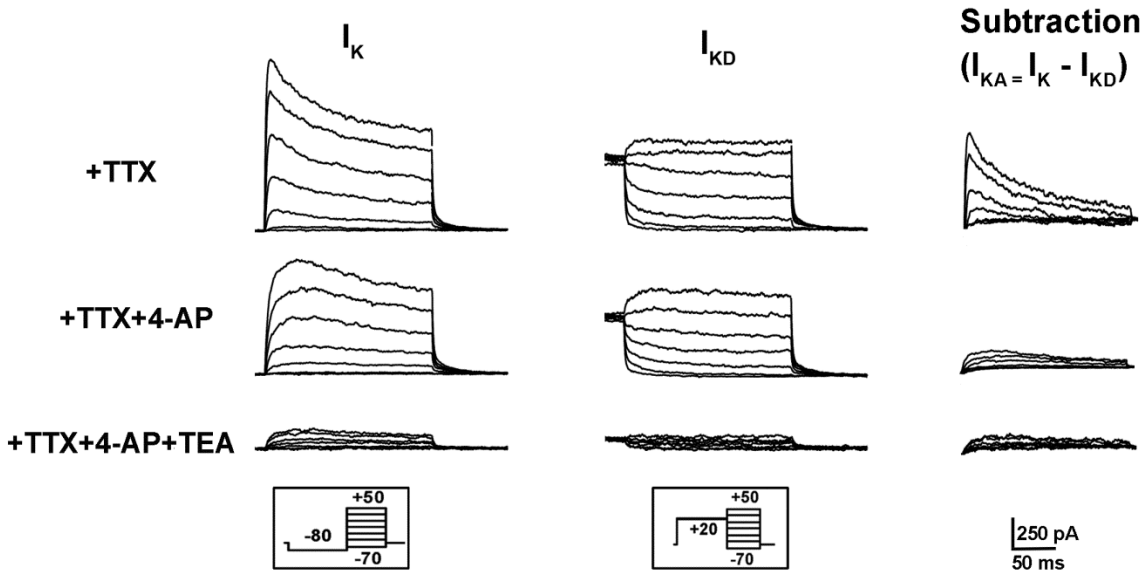

Supplementary Figure 7. Inhibition of IK by potassium channel blockers 4-AP and TEA.

Upper panels, representative tracings showing that the overall IK, IKD and IKA were recorded from a DS neuron in the presence of TTX. Middle panels, representative tracings from the same neuron showing that the IKA component separated by different pre-pulse stimulations was highly sensitive to potassium channel blocker 4-AP. Lower panels, representative tracings from the same neuron showing that another potassium channel blocker TEA further inhibited the remaining IKD in the presence of 4-AP. The similar result was also observed in other four DS and control neurons.

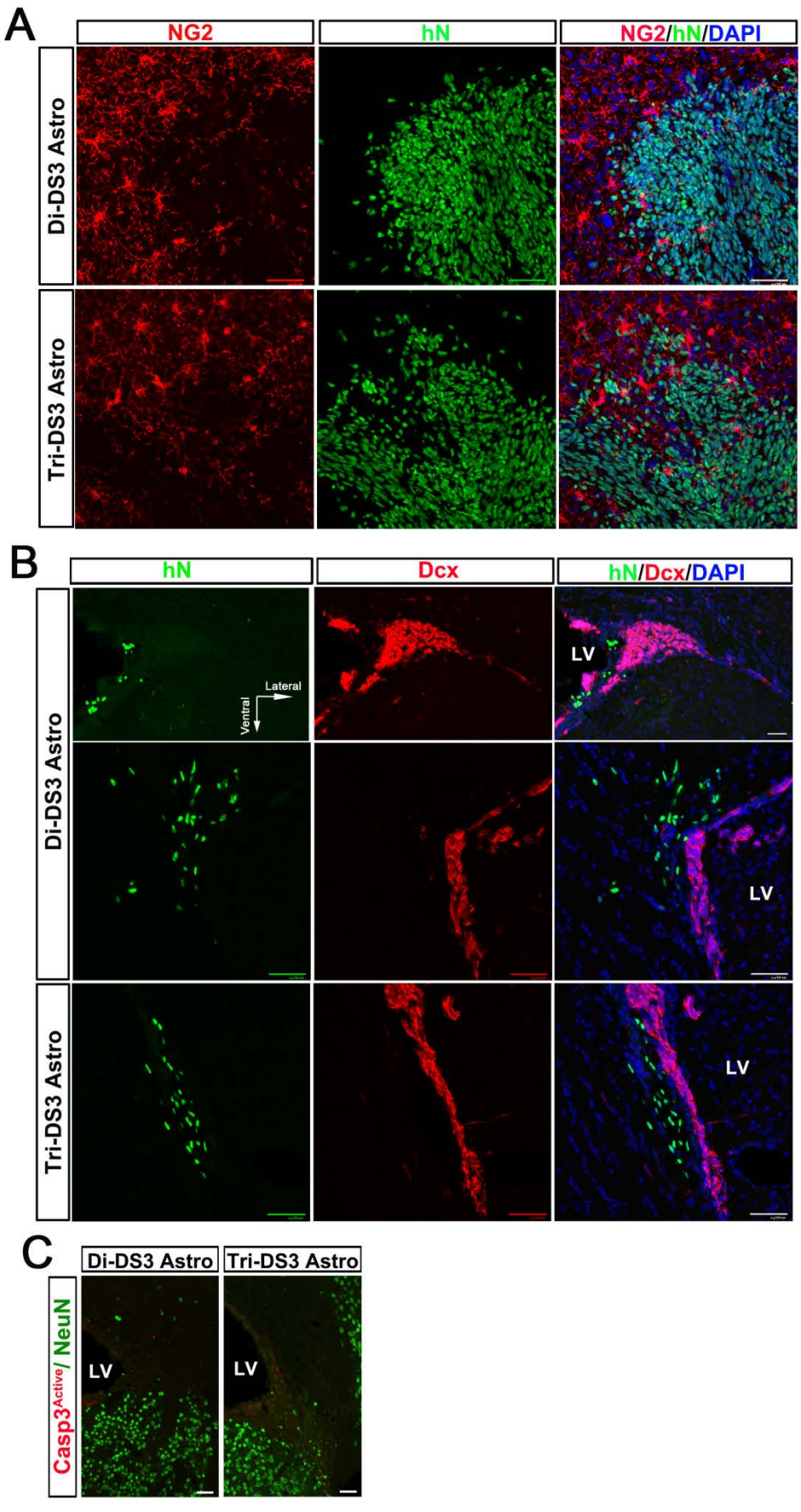
A
NG2
hN
NG2/hN/DAPI
Di-DS3 Astro
Tri-DS3 Astro
B
hN
Dcx
hN/Dcx/DAPI
Lateral
Ventral
LV
Di-DS3 Astro
Tri-DS3 Astro
C
Di-DS3 Astro
Tri-DS3 Astro
Casp3Active/ NeuN
LV

Supplementary Figure 8. The fate of transplanted astroglia and their effects on endogenous neurons.

(A and B) Representatives showing that very few of the transplanted astroglia labeled by hN express NG2, a marker for oligodendroglia progenitor cells and none of them express DCX, a marker for immature neurons. (C) Representatives showing that there is no NeuN+/active caspase3+ neurons in the mouse brain received astroglia transplants. Scale bars represent 50 μm.

Supplementary Table 1.

Basic information of Down syndrome patient fibroblasts from Coriell

Patient no.	Coriell's cat. no.	Sex	Age	Race	Cell type	Karyotype	Generated iPSC lines
DS1	GM04616	Female	3 Days	Caucasian	Fibroblast	47,XX,+21	DS1 iPSCs
DS2	AG08942	Male	21 Years	Caucasian	Fibroblast	47,XY,+21	DS2 iPSCs
DS3	AG06872	Female	1 Year	Caucasian	Fibroblast	47,XX,+21	Di- and Tri-DS3 iPSCs

Supplementary Table 2. Differential expression of gene transcripts in control and DS astroglia.

Symbol	RefSeq #	Fold Change*	Definition
IGF2	NM_001007139.3	83.2801	insulin-like growth factor 2 (somatomedin A)
THBS2	NM_003247.2	32.0389	thrombospondin 2
ADAMTS1	NM_006988.3	12.3143	ADAM metallopeptidase with thrombospondin type 1 motif
THBS1	NM_003246.2	10.0578	thrombospondin 1
CYGB	NM_134268.3	5.8485	cytoglobin
WNT5B	NM_032642.2	5.239	wingless-type MMTV integration site family, member 5B
DKK2	NM_014421.2	4.5819	dickkopf homolog 2
BDNF	NM_001709.3	3.8568	brain-derived neurotrophic factor
DKK3	NM_013253.4	3.8287	dickkopf homolog 3
HMOX1	NM_002133.1	3.5002	heme oxygenase (decycling) 1
BMP1	NM_006129.2	3.3906	bone morphogenetic protein 1
WNT5A	NM_003392.3	3.3129	wingless-type MMTV integration site family, member 5A
FGF1	NM_033136.1	2.9393	fibroblast growth factor 1 (acidic)
APOE	NM_000041.2	2.0003	apolipoprotein E
GPC1	NM_002081.1	1.949	glypican 1
SPARC	NM_003118.2	1.912	secreted protein, acidic, cysteine-rich (osteonectin)
GPC6	NM_005708.2	1.7346	glypican 6
THBS4	NM_003248.3	1.4058	thrombospondin 4
NFE2L1	NM_003204.1	1.3615	nuclear factor (erythroid-derived 2)-like 1
THBS3	NM_007112.3	1.3502	thrombospondin 3
NFE2L2	NM_006164.2	1.2749	nuclear factor (erythroid-derived 2)-like 2
GCLM	NM_002061.2	1.271	glutamate-cysteine ligase, modifier subunit
WNT2B	NM_004185.2	1.2108	wingless-type MMTV integration site family, member 2B
BMP8B	NM_001720.3	1.1686	bone morphogenetic protein 8b
NLGN2	NM_020795.2	1.1229	neuroligin 2
FGF18	NM_003862.1	-1.2347	fibroblast growth factor 18
PRDX1	NM_181696.1	-1.3678	peroxiredoxin 1
PRDX6	NM_004905.2	-1.3868	peroxiredoxin 6
GPX4	NM_002085.2	-1.411	glutathione peroxidase 4 (phospholipid hydroperoxidase)
NQO1	NM_000903.2	-1.5279	NAD(P)H dehydrogenase, quinone 1
NUTF2	NM_005796.1	-1.5302	nuclear transport factor 2
GPC4	NM_001448.2	-1.5863	glypican 4
PRDX2	NM_181738.1	-1.952	peroxiredoxin 2, nuclear gene encoding mitochondrial protein
FGF11	NM_004112.2	-2.0255	fibroblast growth factor 11
GPC2	NM_152742.1	-2.0333	glypican 2
NLGN1	NM_014932.2	-2.1891	neuroligin 1
SPARCL1	NM_004684.2	-2.325	SPARC-like 1 (mast9, hevin)
BMP11 (GDF11)	NM_005811.2	-2.3557	growth differentiation factor 11
PRDX3	NM_006793.2	-2.593	peroxiredoxin 3, nuclear gene encoding mitochondrial protein

GPX3	NM_002084.2	-2.8727	glutathione peroxidase 3
BMP7	NM_001719.1	-3.3932	bone morphogenetic protein 7
BMP6	NM_001718.2	-4.4444	bone morphogenetic protein 6
WNT3	NM_030753.3	-7.6374	wingless-type MMTV integration site family, member 3
BMP5	NM_021073.2	-10.9409	bone morphogenetic protein 5
FGF9	NM_002010.1	-37.037	fibroblast growth factor 9
GPC3	NM_004484.2	-38.1679	glypican 3
NLGN3	NM_018977.2	-95.2381	neuroligin 3
FGF12	NM_004113.3	-97.0873	fibroblast growth factor 12
FGF13	NM_033642.1	-588.2353	fibroblast growth factor 13
WNT3A	NM_033131.2	-714.2857	wingless-type MMTV integration site family, member 3A

Supplementary Table 3. Summary of pathogenic effects of DS astroglia/DS ACM on DS NPCs and neurons.

Reduced neurogenesis	DS NPCs fed with DS ACM gave rise to fewer neurons and more astrocytes, compared to DS NPCs cultured in control ACM.
Reduced neurite outgrowth	Neurons derived from DS NPCs fed with DS ACM showed shorter neurite length than those fed with control ACM.
Delayed neuronal maturation	DS neurons fed with DS ACM showed less robust action potential firings and synaptic activities, compared to DS neurons fed with control ACM.
Increased neuronal apoptosis	DS neurons in DS ACM underwent significant apoptosis.
Minocycline treatment	Improved neuronal neurite outgrowth, survival and maturation of DS neurons

Supplementary Table 4. STR genotyping profile of DS iPSCs and fibroblasts. STRs of all loci for each iPSC match to its corresponding fibroblast line. All iPSC-Fibroblast pairs have matching STR genotyping for the two HSA21 loci, except in the case of the diploid iPSC Di-DS3, where one of the alleles is not seen, consist with the loss of one copy of HSA21.

		Patient DS1						Patient DS2						Patient DS3								
		Fibroblast			DS1 iPSC			Fibroblast			DS2 iPSC			Fibroblast			Tri-DS3 iPSC			Di-DS3 iPSC		
STR Locus	Chr. Location	(CLG16193)			(CLG16121)			(CLG16118)			(CLG16119)			(CLG16122)			(CLG16123)			(CLG16124)		
Amelogenin	Xp22.1–22.3 and Y	X			X			X	Y		X	Y		X			X			X		
TPOX	2p23–2pter	8	11		8	11		9			9			8			8			8		
D3S1358	3p	15	17		15	17		15			15			15	16		15	16		15	16	
FGA	4q28	22	25		22	25		21	24		21	24		20	21		20	21		20	21	
D5S818	5q23.3–32	11	12		11	12		12	13		12	13		11			11			11		
CSF1PO	5q33.3-34	10	12		10	12		11			11			11			11			11		
D7S820	7q11.21–22	8			8			10	11		10	11		10	11		10	11		10	11	
D8S1179	8q	8	13		8	13		12	13		12	13		12	14		12	14		12	14	
TH01	11p15.5	7	9.3		7	9.3		6	9.3		6	9.3		6	9		6	9		6	9	
vWA	12p12–pter	17	18		17	18		17	18		17	18		17	18		17	18		17	18	
D13S317	13q22–q31	9	10		9	10		12	13		12	13		9	11		9	11		9	11	
Penta E	15q	7	10		7	10		11	13		11	13		11	13		11	13		11	13	
D16S539	16q24–qter	11	12		11	12		11			11			9	12		9	12		9	12	
D18S51	18q21.3	12	15		12	15		16	18		16	18		13	14		13	14		13	14	
Penta D	21q	9	11	13	9	11	13	9	12		9	12		9	14	17	9	14	17	9	17	
D21S11	21q11–21q21	28	29		28	29		28	31	32.2	28	31	32.2	30	31.2	32.2	30	31.2	32.2	31.2	32.2	

Supplementary Table 5.

Quantitative PCR primers

Gene	Forward sequence	Reverse sequence	Length (bp)
GFAP	AGTCCCTGGAGAGGCAGATGCGC GAGC	ATGTTCCTCTTGAGGTGGCCTTCTGAC	313
NFE2L2	TGATTGACATACTTTGGAGGC	TCTTCATCTAGTTGTAACTGAGCG	181
TSP1	GCTGCACTGAGTGTCACTGTC	TCAGGAACTGTGGCATTGG	91
TSP2	GTGCAGGAGCGTCAGATGT	GGGTTGGATAAACAGCCATC	62
GAPDH	GAGTCCACTGGCGTCTTCAC	TTCACACCCATGACGAACAT	119

Supplementary Table 6.

Taqman primers

Gene	Gene expression assay catalog number
GLAST	Hs00188193_m1
GLT-1	Hs01102423_m1
S100B	Hs00902901_m1
iNOS	Hs01126940_gH
GAPDH	Hs02758991_g1